Water Research 216 (2022) 118339

Contents lists available at ScienceDirect

Water Research

journal homepage: www.elsevier.com/locate/watres

Dynamic alpha factors: Prediction in time and evolution along reactors

Dániel Bencsik [a,b,*], Imre Takács [a,c], Diego Rosso [c,d]

[a] Dynamita, SARL, 2015 route d'Aiglun, Sigale 06910, France
[b] National University of Public Service, 2 Ludovika tér, Budapest H-1083, Hungary
[c] Water-Energy Nexus Center, University of California Irvine, Irvine, CA 92697-2175, United States
[d] Civil and Environmental Engineering Department, University of California Irvine, Irvine, CA 92697-2175, United States

ARTICLE INFO

Keywords:
Alpha factor
Dynamic modelling
Benchmark simulation model
Aeration
Wastewater

ABSTRACT

The performance of aeration – one of the most costly processes at water resource recovery facilities – is heavily impacted by actual wastewater characteristics which are commonly taken into account using the alpha factor (α). This factor varies depending on hydraulic and organic loading; such variance includes both time and spatial fluctuations. In standard design practice, it is often considered as a fixed number, or at best, a predefined time series. The objective of this paper is to propose a new method of predicting plantwide trends in the α factor through the use of process modelling which can accommodate diurnal and seasonal variations. The authors' concept takes into account the dependence of α on sludge retention time in the form of degradation kinetics, the effects of organic loading (influent filtered COD), the presence or absence of anoxic zones, diffuser depth, and the impact of high MLSS found in certain, e.g., MBR, technologies. The developed model was calibrated using data from numerous facilities, relying on off-gas measurements and tests in clean and process water. Model validation was carried out against averaged α factor gradient data from one plant, and against diurnal air flow measurements from another. The Benchmark Simulation Model 1 configuration was used to demonstrate the applicability of the proposed model – in estimation of blower energy consumption and peak air flow requirements – comparing it with constant and scheduled α factor-based approaches.

1. Introduction

Wastewater aeration is one application of gas-transfer theory, and it is necessary for design and the analysis of aerobic processes. One of the bottlenecks impeding the accurate application of gas-transfer theory is the step between clean gas transfer scenarios (e.g., air and clean water) and contaminated scenarios (e.g., air and wastewater), but due to the unknown composition of the many contaminants that are present in wastewater, accuracy is limited. Numerous investigators have been studying how to quantify and predict the effect of contaminants on gas transfer for the better part of the last century (since Kessener and Ribbius, 1934 and Eckenfelder and Barnhart, 1961). The dynamic nature of gas-liquid mass transfer significantly impacts the actual process air requirements of water resource recovery, affecting operational costs. It also plays a role in equipment sizing and capital costs, thus defining peak air demand.

Aeration systems are specified based on clean water performance (defined as Standard Oxygen Transfer Efficiency, SOTE, %; Standard Oxygen Transfer Rate, SOTR, $kg_{O2,transferred}\ h^{-1}$), and they are scaled to process conditions using the α factor (dimensionless) as well as the diffuser fouling factor (F, dimensionless) to quantify the decline of performance with time in operation (U.S. Environmental Protection Agency – USEPA, 1989). During the design stage, the quantification of SOTE is the responsibility of the aeration system manufacturer and an independent witness. The quantification of α and F are the purview of the design engineers. Standard testing protocols for SOTE quantification are adopted in design (American Society of Civil Engineers – ASCE, 2018), reducing the uncertainty of SOTE quantification to the experimental error. However, the research and corresponding literature on the subject of α and F quantification still fall short of significantly reducing uncertainty. This shortcoming is not due to negligence, but to the nature of the definition of α and F. The former is the ratio of oxygen transfer in process water vs. clean water (i.e., αSOTE/SOTE), aggregating in one parameter (or variable) all the uncertainty on the composition of the carbonaceous load applied to the process. The latter is site-specific and depends on a multitude of factors given that it is a factor that aggregates biofilm adhesion and growth, inorganic scaling, and diffuser material degradation (U.S. Environmental Protection Agency – USEPA, 1989; Kim and Boyle, 1993; Wagner and Pöpel, 1998; Gillot et al., 2005; Rosso

* Corresponding author at: National University of Public Service, 2 Ludovika tér, Budapest H-1083, Hungary.
E-mail address: daniel@dynamita.com (D. Bencsik).

https://doi.org/10.1016/j.watres.2022.118339
Received 25 October 2021; Received in revised form 2 March 2022; Accepted 18 March 2022
Available online 21 March 2022

Nomenclature

α	alpha (wastewater/clean water) factor
αF	alpha factor for aged diffusers
αFSOTE	standard oxygen transfer efficiency in process water for aged diffusers [%]
bCOD	biodegradable chemical oxygen demand [g_{COD} m^{-3}]
$coeff_{damp,ALPHA}$	coefficient of alpha first order limitation-dampening term
$corr_{cw,SCCOD,ALPHA}$	clean water correction term in filtered COD-alpha indicator correlation
$corr_{hdiff,\alpha}$	depth-related alpha factor correction term
$corr_{TSS,\alpha}$	solids-related alpha factor correction term
$damp_{ALPHA}$	alpha first order limitation-dampening term
$exp_{cw,SCCOD,ALPHA}$	clean water exponent of filtered COD-alpha indicator correlation [m^3 g_{COD}^{-1}]
F	diffuser fouling factor
$f_{O2,max,ALPHA}$	non-aerated zone alpha improvement rate increase
h_{diff}	diffuser submergence [m]
$K_{I,SCCOD,ALPHA}$	half-value in filtered COD-alpha indicator correlation [g_{COD} m^{-3}]
$K_{O2,ALPHA}$	half-saturation of dissolved oxygen for alpha rate [g_{O2} m^{-3}]
$max_{ww,SCCOD,ALPHA}$	maximum of filtered COD-alpha indicator correlation, wastewater
MCRT	mean cell retention time [d]
$min_{SCCOD,ALPHA}$	minimum of filtered COD-alpha indicator correlation
nbCOD	non-biodegradable chemical oxygen demand [g_{COD} m^{-3}]
$pow_{damp,ALPHA}$	power of alpha first order limitation-dampening term
Q	volumetric flow of wastewater [m^3 d^{-1}]
q_{ALPHA}	alpha improvement rate [m^3 g_{VSS}^{-1} d^{-1}]
$q_{ALPHA,O2}$	dissolved oxygen-corrected alpha improvement rate [m^3 g_{VSS}^{-1} d^{-1}]
Q_{SALPHA}	load of alpha indicator [m^3 d^{-1}]
$rateQ_{SALPHA}$	reaction rate of alpha indicator in volumetric unit [m^3 d^{-1}]
$rate_{SALPHA}$	reaction rate of alpha indicator [d^{-1}]
rbCOD	readily biodegradable chemical oxygen demand [g_{COD} m^{-3}]
r_{SALPHA}	process rate for elimination of surfactants [d^{-1}]
S_{ALPHA}	alpha indicator
$S_{ALPHA,sat}$	maximum alpha indicator
SCCOD	filtered (soluble + colloidal) chemical oxygen demand [g_{COD} m^{-3}]
$sl_{hdiff,\alpha}$	slope of depth-related alpha factor correction term [m^{-1}]
$sl_{SCCOD,ALPHA}$	slope of filtered COD-alpha indicator correlation [m^3 g_{COD}^{-1}]
$sl_{TSS,\alpha}$	slope of solids-related alpha factor correction term [m^3 kg_{TSS}^{-1}]
S_{O2}	dissolved oxygen concentration [g_{O2} m^{-3}]
SOTE	standard oxygen transfer efficiency [%]
V_r	reactive volume [m^3]
v_{SALPHA}	stoichiometric coefficient for alpha indicator (in elimination of surfactants)
X_{TSS}	total suspended solids concentration [g_{TSS} m^{-3}]
X_{VSS}	volatile suspended solids concentration [g_{VSS} m^{-3}]

and Stenstrom, 2006a; Garrido-Baserba et al., 2016; 2017; 2018; Rosso, 2018).

Fig. 1. illustrates an example of how the contribution of factors can be parsed out. Nevertheless, the oxygen transfer operations in a wastewater treatment plant include the compounding effect of all these combined factors (α•F•SOTE = αFSOTE), thereby forcing investigators and design engineers to parse the individual contributions of said factors, chiefly because the responsibility of each is attributed to different

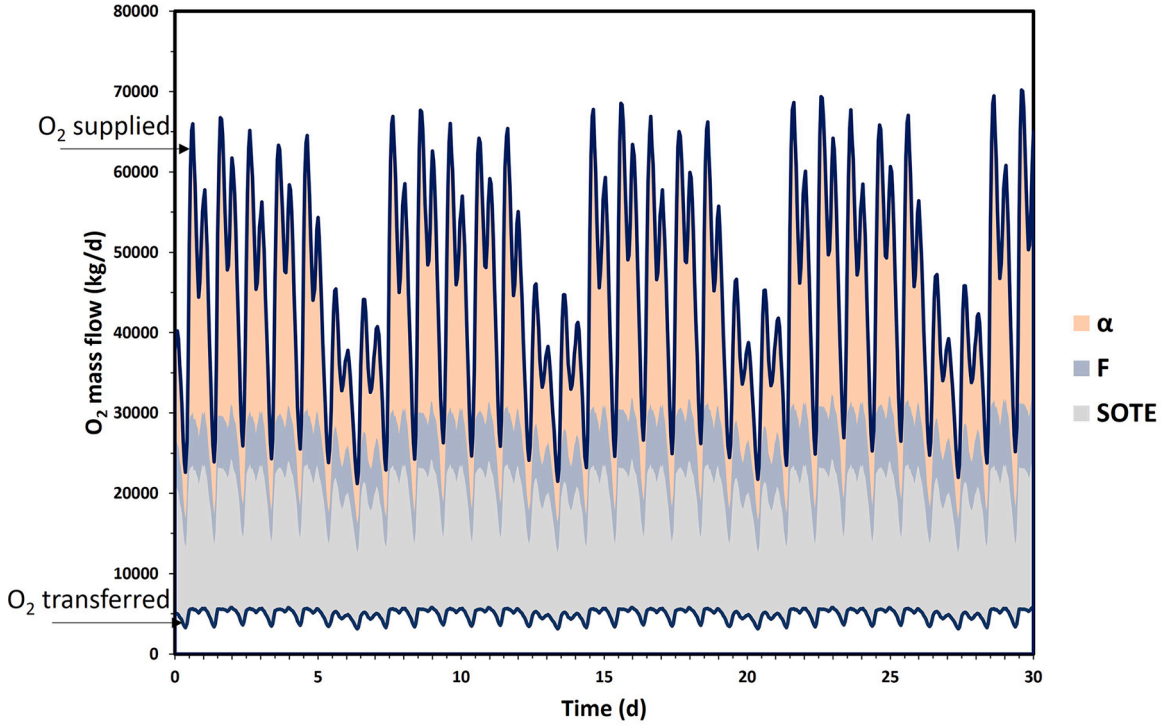

Fig. 1. Illustration of clean and process water factors contributing to oxygen transfer limitations.

parties in design (Rosso, 2018).

Note the significant difference in dynamics amongst these variables, with F being the least varying and α the most varying over the short term.

Studying the illustrated example, it is apparent that the so-called α factor can be the most significant barrier to oxygen dissolution and also the most sensitive to varying loading circumstances (Karpinska and Bridgeman, 2016) which, among diurnal patterns, also show contrast between workdays and weekends. The background of this factor relates to contaminants in the wastewater and different aerators in conjunction with links between surfactants and bubble size which have long been studied (*inter alia,* Kessener and Ribbius, 1934; Stenstrom and Gilbert, 1981).

The α factor is known to be related to the mean cell retention time (MCRT) of a treatment plant (U.S. Environmental Protection Agency – USEPA, 1989; Rosso et al., 2005; Gillot and Héduit, 2008) due to kinetic requirements of the processes responsible for eliminating constituents that hamper oxygen transfer. This causes α to vary with hydraulic loading which is inversely proportional to the dynamic MCRT. Consequently, the greater the internal recirculation applied to a train, the flatter its α gradient will be due to the load distribution effect which also reduces the need for diffuser tapering (Rosso et al., 2007).

The presence of non-aerated selectors at a treatment line can improve α values overall. This is because surface-active agents tend to accumulate at bubble surfaces, and therefore are harder to access and degrade. Aerobic processes that directly utilize O_2 as an electron acceptor are prone to this effect (Rosso and Stenstrom, 2006b, 2007).

Diffuser submergence plays a role, too, on the local α in aerated tanks (Gillot and Héduit, 2008), as the accumulation of surfactants at bubble surfaces – toward a steady-state in forming a barrier film – is facilitated by longer bubble contact times (Doyle et al., 1983; Wagner and Pöpel, 1996).

Experience shows that oxygen transfer clearly declines with increasing organic contaminant loading, and this has been linked with a relation of α factor and soluble COD as well as colloidal COD concentration (Mueller et al., 2000; Odize et al., 2016).

With increased solids concentrations in reactors, α reduces locally due to the increased viscosity and non-Newtonian nature of the mixed liquor, and thus drives bubble coalescence which is especially discernible in the range of operating MLSS of membrane bioreactors or aerobic digesters (Muller et al., 1995; Krampe and Krauth, 2003; Steele et al., 2019). Below 4 kg TSS m^{-3}, though, facilities typically operate at shorter MCRT and lower MLSS, and the resulting α factor is a function of the surfactant available for accumulation at the gas-liquid interface (Baquero-Rodríguez et al., 2018).

Efforts have previously been made to describe the α factor's dynamic nature, relying on algebraic correlations. The first examples of such efforts include prediction in function of MCRT, air flux, and submergence (Rosso et al., 2005; Gillot and Héduit, 2008). One case included the additional impact of MLVSS along with MCRT in the equation applied (Henkel et al., 2011). Other methods incorporated a direct negative correlation to total COD or soluble COD (Jiang et al., 2017; Boog et al., 2020; Ahmed et al., 2021).

The available empirical models may prove useful in estimating a plant-average α factor. Yet, α also varies per reactor and along each reactor, analogously to the oxygen uptake, since both are driven by process loading. However, α and OUR are not correlated because their dynamics are affected by different causes: whereas OUR is driven by the entire biodegradable COD and ammonia load, α is mainly affected by a small subset of the bCOD molecules, i.e. the surface-active agents (Odize et al., 2016).

However, past work did not address the kinetic and mass balance-related phenomena that, in fact, determine the location-specific trend and time-based changes regarding the α factor. The complex effects of environmental and operational conditions are fundamental in predicting this factor for the accurate design and operation of WRRFs (Amaral et al., 2019).

The goal of this paper is to propose a novel approach that incorporates rate equations into process models based upon a surrogate state variable to simulate the wide range of contributors to α while adjusting to diurnal and seasonal variations in hydraulic and organic loading.

2. Methodological approach

The proposed concept of dynamic α factor prediction is based on a "typical" or "average" degradable and surface-active component. As this component sorbs onto flocs and degrades along the process, α increases as depicted in Fig. 2. in a simple conceptual form. This new concept was selected because variations of the α value in space and time cannot be directly linked to any of the state variables (readily biodegradable substrate, ammonia, etc.) usually included in process models.

To quantify the effect of surface-active agents in individual bioreactors and reactive compartments, this paper reconsiders the previous dynamic definition of α as a function of COD or bCOD (Jiang et al., 2017; Boog et al., 2020; Ahmed et al., 2021), introducing a state variable named "alpha indicator" (S_{ALPHA}). This unitless indicator is dedicated specifically to consider the loading of oxygen transfer-impeding contaminants to individual process units in treatment plants, and their transformation within those units that incorporate biokinetic and other reactions. The change of alpha indicator in time within a completely stirred tank is described by a component balance according to Eq. (1):

$$\frac{dS_{ALPHA}}{dt} = \frac{Q_{S_{ALPHA,in}} - Q_{S_{ALPHA,out}} + rateQ_{S_{ALPHA}}}{V_r} \quad (1)$$

The load of alpha indicator to a tank is given by Eq. (2).

$$Q_{S_{ALPHA,in}} = Q_{in} \cdot S_{ALPHA,in} \quad (2)$$

Similarly, the flow of alpha indicator leaving a tank is interpreted in the form of Eq. (3).

$$Q_{S_{ALPHA,out}} = Q_{out} \cdot S_{ALPHA} \quad (3)$$

The kinetic reaction rate of the alpha indicator regarding the removal process of surfactants, present as $rate_{SALPHA}$ in Eqs. (4) and (5), is calculated like a rate expression of any integrated state variable derived from a biokinetic matrix by multiplying a stoichiometric coefficient (ν_{SALPHA} with a value of 1, as it indicates a positive change of the indicator towards a saturation value acting as asymptote) by a process rate (r_{SALPHA}):

$$rateQ_{S_{ALPHA}} = V_r \cdot rate_{S_{ALPHA}} \quad (4)$$

$$rate_{S_{ALPHA}} = \nu_{S_{ALPHA}} \cdot r_{S_{ALPHA}} \quad (5)$$

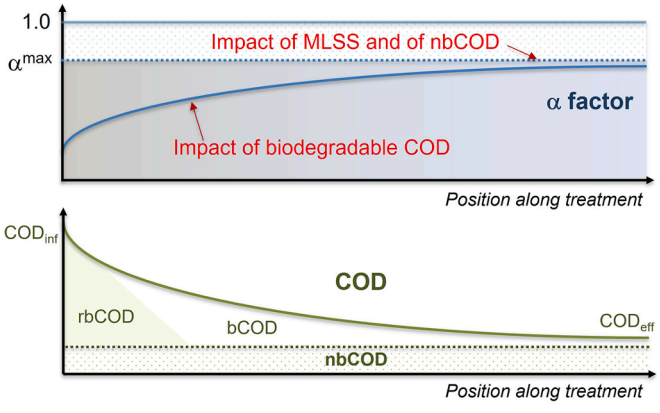

Fig. 2. Concept drawing of contribution of different contaminants to α as it evolves along the treatment process, analogously to a certain fraction of COD.

The process rate (regarding the elimination of surfactants, calculated by Eq. (6)) depends on an alpha improvement rate component ($q_{ALPHA,O2}$) which is correlated with the MLVSS concentration, meaning that the longer the water is in contact with the sludge, the larger change can be achieved in the alpha indicator. This correction is in agreement with the observations previously reported by multiple investigators, i.e. that α improves with increasing MLVSS for activated sludge processes (Rosso et al., 2005; Gillot and Héduit, 2008). This correction is needed to account for the benefits of biomass sorption of surfactants. The driving force of the change in alpha indicator is determined by the difference of the alpha indicator's saturation value (1 by default, representing the clean water value) and the actual value of the indicator, further corrected by a dampening term (described in Eq. (8)).

$$r_{S_{ALPHA}} = q_{ALPHA,O_2} \cdot X_{VSS} \cdot damp_{ALPHA} \cdot \left(S_{ALPHA,sat} - S_{ALPHA}\right) \quad (6)$$

The $q_{ALPHA,O2}$ component of the process rate is derived from the kinetic model parameter q_{ALPHA}, which must be corrected by the inverse DO saturation term in Eq. (7) in order to account for the enhancing effect of anaerobic or anoxic conditions on the α factor. This factor addresses the beneficial effects of anoxic reactors in sorbing surfactants that otherwise would accumulate on bubbles (Rosso and Stenstrom, 2006b; 2007). Thus, $q_{ALPHA,O2}$ is highest at 0 $mg_{O2}\ l^{-1}$ and declines towards q_{ALPHA} with increasing aerated status:

$$q_{ALPHA,O_2} = q_{ALPHA} \cdot \left(\left(1 - f_{O_2,max,ALPHA}\right) \cdot \frac{S_{O_2}}{K_{O_2,ALPHA} + S_{O_2}} + f_{O_2,max,ALPHA} \right) \quad (7)$$

The so-called dampening is implemented – in the form of Eq. (8) – because the improvement in α factor with sludge residence time does not, in fact, occur according to first order saturation kinetics. Above a certain ratio of alpha indicator to the saturation value, the alpha improvement rate shall be justified by the dampening term to compensate for the otherwise hyperbolic increase in the indicator toward the saturation number.

$$damp_{ALPHA} = 1 + coeff_{damp,ALPHA} \cdot \frac{S_{ALPHA}}{S_{ALPHA,sat}}^{pow_{damp,ALPHA}} \quad (8)$$

The α factor itself is actually a variable calculated from the alpha indicator according to Eq. (9) in order to be able to account for local differences in depth and MLSS concentration using their respective correction terms:

$$\alpha = S_{ALPHA} / corr_{h_{diff},\alpha} \cdot corr_{TSS,\alpha} \quad (9)$$

In theory, the model's alpha indicator represents a steady-state effect of surfactants forming a barrier at bubble interfaces, so the α factor – relevant to a given submergence – needs to be back-calculated from the indicator using the depth correction term shown by Eq. (10).

$$corr_{h_{diff},\alpha} = (S_{ALPHA} - 1) \cdot e^{sl_{h_{diff},\alpha} \cdot h_{diff}} + 1 \quad (10)$$

The effect of MLSS on the α value is not related directly to surfactants, so it is handled separately from the biokinetic changes that play a role in the alpha indicator. An exponential correction term accounts for this based on Eq. (11). The slope of this correction ($sl_{TSS,\alpha}$) shall be different for coarse bubble aerators, and in this way the model can account for their higher flow regime interfaces – and associated α factors – compared to fine bubble diffusers (Stenstrom and Gilbert, 1981; Rosso et al., 2006b).

$$corr_{TSS,\alpha} = e^{sl_{TSS,\alpha} \cdot X_{TSS}} \quad (11)$$

Values of the alpha indicator are associated with feed streams to simulate their surfactant content. Clean water is described with an alpha indicator of 1. For the influent wastewater, a double exponential function – as seen in Eq. (12) – represents the relationship of the alpha indicator in terms of influent filtered COD.

$$S_{ALPHA} = \frac{max_{ww,SCCOD,ALPHA} - min_{SCCOD,ALPHA}}{1 + e^{\left(SCCOD - K_{I,SCCOD,ALPHA}\right) \cdot sl_{SCCOD,ALPHA}}} + min_{SCCOD,ALPHA} + corr_{cw,SCCOD,ALPHA} \quad (12)$$

As a method of accounting for dilute wastewater samples, the exponential clean water correction term in Eq. (13) is added to the inverse sigmoid-type base function.

$$corr_{cw,SCCOD,ALPHA} = \left(1 - max_{ww,SCCOD,ALPHA}\right) \cdot e^{-exp_{cw,SCCOD,ALPHA} \cdot SCCOD} \quad (13)$$

For demonstrating modelling applications, a variant of the BSM1 test configuration (Alex et al., 2008) was set up in the Sumo21 simulation software and used to evaluate potential CAPEX and OPEX savings by using the predictive α method (and the resultingly more accurate blower size, control strategy, and power demand) instead of fixed or scheduled α values generally used in design.

For the sake of the case studies in this paper, there were some modifications necessary compared to the original BSM1 model setup. The double exponential settler implementation (Takács et al., 1991) was replaced with a triple exponential approach and compression was included (Dynamita, 2021). Furthermore, no sensor delays were added because they are not significant for the purpose of these studies. All three compartments of the BSM1 reactor cascade were set up with DO control and assigned set points of 2 $mg_{O2}\ l^{-1}$ given that the standard BSM1 version provides over-aeration with the predefined $\alpha \cdot k_La$ values (10 h^{-1} for the first two of the three aerobic zones). After initial model testing, it was decided that DO probes in the three aerated cells and controlled air valves are cheaper compared to purchasing bigger blowers to meet the significant loading peaks and over-aerating the first two cells in lower loaded periods that are present in BSM1. DO set points were constant throughout the simulation runs. For these example studies, there is effluent discharge limitation assigned for ammonia nitrogen, i.e., 1.0 $mg_N\ l^{-1}$ as weekly average and a maximum daily peak of 4.0 $mg_N\ l^{-1}$. Since this paper focuses on aerated processes, optimizing the effluent TN via denitrification was not an objective.

The selected biokinetic model was also replaced from the original ASM1 by MiniSumo in favour of the available gas transfer background calculations along with Sumo21's blower and pump models to assess energy and associated costs (Dynamita, 2021). MiniSumo is a simplified plant-wide model with one-step nitrification and denitrification, focusing on estimating oxygen requirement and sludge production. Its gas transfer concept relies on Fick's two-film theory and Henry's law, and features equipment models of fine and coarse bubble diffuser types for SOTE prediction. Air flow rates are standardized at 20°C temperature and 1 atm pressure. Throughout the model simulation, α factor for aged diffusers (αF, including the fouling factor F (U.S. Environmental Protection Agency – USEPA, 1989)) was used to interpret results – having assigned a fixed value of 0.75 for F. The selection of a constant F is adequate if the modelling time-window is limited (e.g., less than 1-2 months). In practice, this is best adjusted knowing the diffuser age and the time of the last cleaning procedure (Jiang et al., 2020).

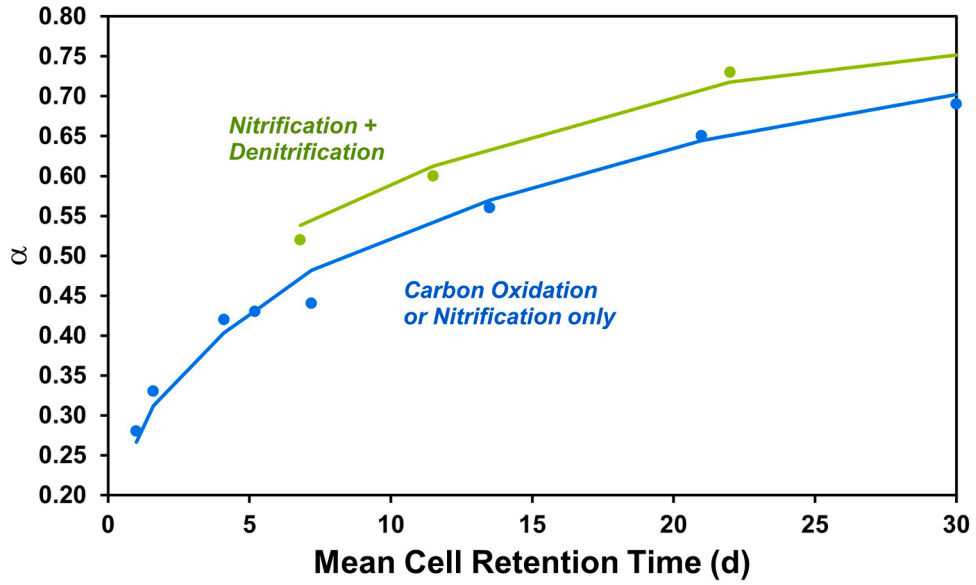

Fig. 3. Model calibration regarding α factor versus MCRT. The data used here is from plants with Mediterranean climate.

3. Model calibration and validation

Data was collected from results of off-gas measurement campaigns, batch clean water, and process water tests as well as from aeration literature review (Doyle et al., 1983; Gillot and Héduit, 2008; Leu et al., 2009; Baquero-Rodríguez et al., 2018). Reconciliation of data was carried out according to the IWA Good Modelling Practice Guidelines (Rieger et al., 2013). The model was then first fitted to averaged α factor off-gas measurements (American Society of Civil Engineers – ASCE, 2018) from facilities applying newly commissioned fine pore diffusers – with and without non-aerated selectors – in function of the given plant MCRT values, as displayed in Fig. 3. The depth-related, as well as solids-related corrections in the model, were fine-tuned based upon clean water and process water unsteady state test results (American Society of Civil Engineers – ASCE, 2006; 2018). The α versus influent filtered COD relationship was adjusted based on air flow-weighted average diurnal off-gas measurements (American Society of Civil Engineers – ASCE, 2018) from a facility in Simi Valley, California (Leu et al., 2009), as shown by Fig. 4 which displays a uniform distribution of errors

Table 1
Calibrated model parameter set.

Parameter symbol	Value	Unit
$coeff_{damp,ALPHA}$	4.2	–
$exp_{cw,SCCOD,ALPHA}$	0.05	$m^3\ g_{COD}^{-1}$
$f_{O2,max,ALPHA}$	2.5	–
$K_{O2,ALPHA}$	0.05	$g_{O2}\ m^{-3}$
$K_{I,SCCOD,ALPHA}$	162	$g_{COD}\ m^{-3}$
$max_{ww,SCCOD,ALPHA}$	0.5	–
$min_{SCCOD,ALPHA}$	0	–
$pow_{damp,ALPHA}$	7.3	–
q_{ALPHA}	0.0014	$m^3\ g_{VSS}^{-1}\ d^{-1}$
$sl_{SCCOD,ALPHA}$	0.067	$m^3\ g_{COD}^{-1}$
$sl_{hdiff,\alpha}$	-0.29	m^{-1}
$sl_{TSS,\alpha}$ (fine bubble)	-0.0711	$m^3\ kg_{TSS}^{-1}$
$sl_{TSS,\alpha}$ (coarse bubble)	-0.0474	$m^3\ kg_{TSS}^{-1}$

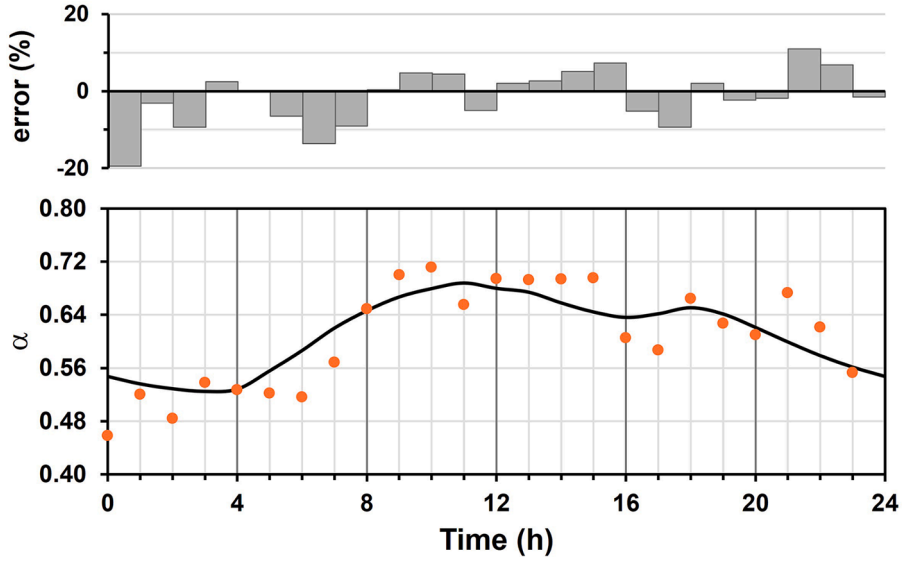

Fig. 4. Model calibration for α profile against time-dependent organic loading.

between measured and modelled outputs throughout the day. Dots on graphs indicate measured data, while connected lines represent model outputs. Calibrated model parameter values are listed in Table 1.

Model validation was carried out against measurements from two water resource recovery facilities. Firstly, steady-state α factor simulations were compared to daily averaged off-gas test (American Society of Civil Engineers – ASCE, 2018) results from a municipal plant located in Southern California (not the aforementioned plant used for calibration), with two parallel and independent lines fed separate return sludge (Rosso et al., 2007). Both were equipped with ceramic disc diffusers and received the same influent quality but with different volumetric loading; thus, one of them was operated as a BOD removal system (i.e., carbon oxidation only, with short sludge retention time), while the other one also featured nitrification (i.e., with long sludge retention time). Throughout the sampling locations, measured data points are somewhat scattered compared to a continuous gradient due to the tank hydrodynamic conditions that are difficult to mimic in process modelling – this is especially true of the low α measurements at the effluent of both systems, and the high outlying datapoints between 130 and 200 m positions of the high MCRT system. Regardless of this, the estimated α trend presented by Fig. 5 shows good agreement with the measured data, reproducing the phenomenon that higher MCRT can result in a two-fold increase in oxygen transfer efficiency (Rosso et al., 2005; Gillot and Héduit, 2008). Replicating such evolution of α along reactors, as well as quantifying air distribution accurately when setting up a plant model, are key aspects of diligent plant-wide oxygen transfer modelling. Also, these are required for reliable energy and cost calculations and are aligned with the various degrees of oxygenation requirements at different stages of treatment.

Secondly, the capability of estimating dynamically varying air flow demand was tested based on a 2-day dataset – as seen on Fig. 6 – from a plug flow reactor of WWTP Waßmannsdorf in Brandenburg, Germany, a facility with denitrification and enhanced biological phosphorus removal (Schuchardt et al., 2007). Three zones of the aeration tank – with DO control in each, utilizing a ceramic tube diffuser system – were used for comparison. Modelled results show satisfactory response in terms of air flow.

Despite the slightly higher modelled air flow during the peak loading period, a need for larger or more blowers in practice may not be needed if the exercise of scheduling blower operations with varying diurnal DO set points is applied. Being able to reproduce such dynamic profiles along with α in various reactors is essential for the specification of blowers and for the determination of the blower duty schedule. Also, since the n+1 blower added to operations could incur stiff power demand penalties, there is a need to overlay these dynamic calculations with the structured power tariff to increase the accuracy of predicting energy consumption, power demand, energy costs, and carbon footprint (Aymerich et al., 2015; Amerlinck et al., 2016; Emami et al., 2018).

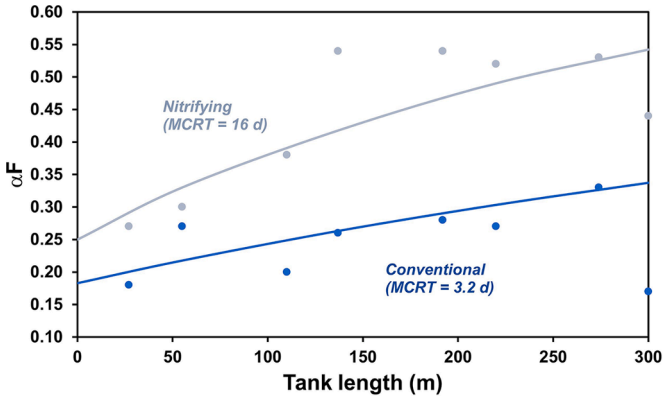

Fig. 5. Model validation with plug-flow αF gradients.

5. Results and discussion

In the first example, the model test configuration ran at a steady-state in dry weather conditions, using Sumo21's combined global and local solvers, followed by five weeks of repeated dry weather diurnal weeks. Three runs were performed (Fig. 7) to obtain the weekly blower energy demand for the following design scenarios:

1 "Predictive scenario": Kinetic-based model prediction (space and time varying αF): average calculated αF at 0.49, 0.52 and 0.53 in AER1, AER2 and AER3
2 "Cautious scenario": design based on constant αF set to 0.3, 0.4 and 0.5 in AER1, AER2 and AER3
3 "Optimistic scenarios": design based on constant αF set to 0.5, 0.6 and 0.7 in AER1, AER2 and AER3.

Compared to the cautious design example that estimates an accumulated blower energy consumption of 44.5 MWh, the time and location-specific αF prediction use case determines 33.3 MWh, suggesting 25 % savings on operational costs if blowers with adequate turn-down capability were specified. The required blower capacity determined with predicted αF is also lower by 21 % ($1.08\ 10^4\ m^3\ h^{-1}$ instead of $1.37\ 10^4\ m^3\ h^{-1}$), with corresponding implications on CAPEX and OPEX. Although the weekend air demand estimated by the optimistic design approach shows good agreement with the predictive method, it only assumes 30.7 MWh of required blower energy and $8.30\ 10^3\ m^3\ h^{-1}$ for the peak air flow requirement which would lead to insufficient air supply during most of the week.

Overall, the results and the illustration in Fig. 7 emphasize that, since predictive αF values relate to dynamic process variables that respond to fluctuations in load, the corresponding air flow calculation also follows turn-down and turn-up trends (bounded by the optimistic and cautious αF-based ranges) that blowers experience in actual facilities.

The following case study was developed to show the negative effects on effluent quality from choosing excessively optimistic values of αF. Two simulations were run for 5 weeks with dry weather diurnal flows following steady-state calculation. All runs applied the predictive αF method, however, the blower size was restricted according to the capacity determined from either the previously presented predictive scenario ($1.08\ 10^4\ m^3\ h^{-1}$), the cautious scenario ($1.37\ 10^4\ m^3\ h^{-1}$) or the optimistic design scenario ($8.30\ 10^3\ m^3\ h^{-1}$) in order to simulate a real plant situation. The total air flow was distributed assuming manual butterfly valves in the proportion of 53 %, 29 %, and 18 % to the three aerated zones (AER1 to AER3). Fig. 8 displays a comparison of the resulting DO levels in the last aerated cell (AER3) and NH_4-N concentrations in the plant effluent.

Despite the smaller blower size and associated cost benefit shown by optimistic αF-based sizing, this method confirms how excessively optimistic α ranges correspond to inevitably insufficient air flow requirements during periods with higher load, i.e., when oxygen is most needed, and with DO targets only met throughout the weekend (on some days, the actual DO drops as low as $0.5\ mg_{O2}\ l^{-1}$). Moreover, this even leads to daily maximum effluent NH_4-N violations on the first three consecutive days (barely complying with the $1\ mg_N\ l^{-1}$ weekly average limitation), possibly leading to significant fines. Effluent limitations can only be met with the predictive method, or the cautious approach – the latter, however, entails the requirement of higher aeration capacity that impacts costs, as discussed in Fig. 7.

With regard to the second demonstrated case, dynamically predicted αF numbers take into account variations in a real plant that the underlying kinetic process variables are adapted to, and when linked to a biokinetic model, they are efficient in determining whether an aeration system is appropriately sized to comply with environmental standards. As portrayed in Fig. 8, predicting αF can also be coupled with increased accuracy in blower design, which in this case corresponds to reduced blower capacity, to evaluate cases when the phenomenon of DO sag (due

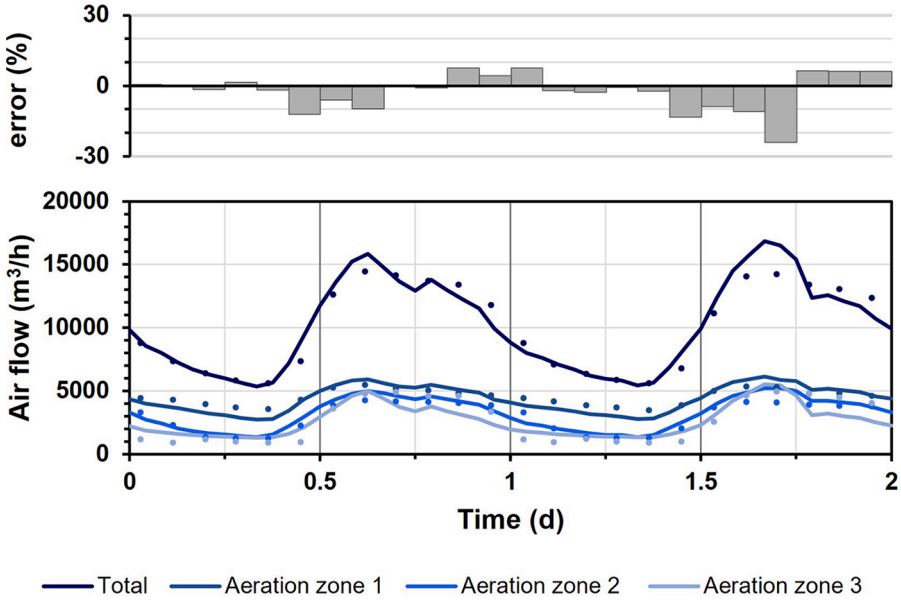

Fig. 6. Model validation with dynamic air flow profiles.

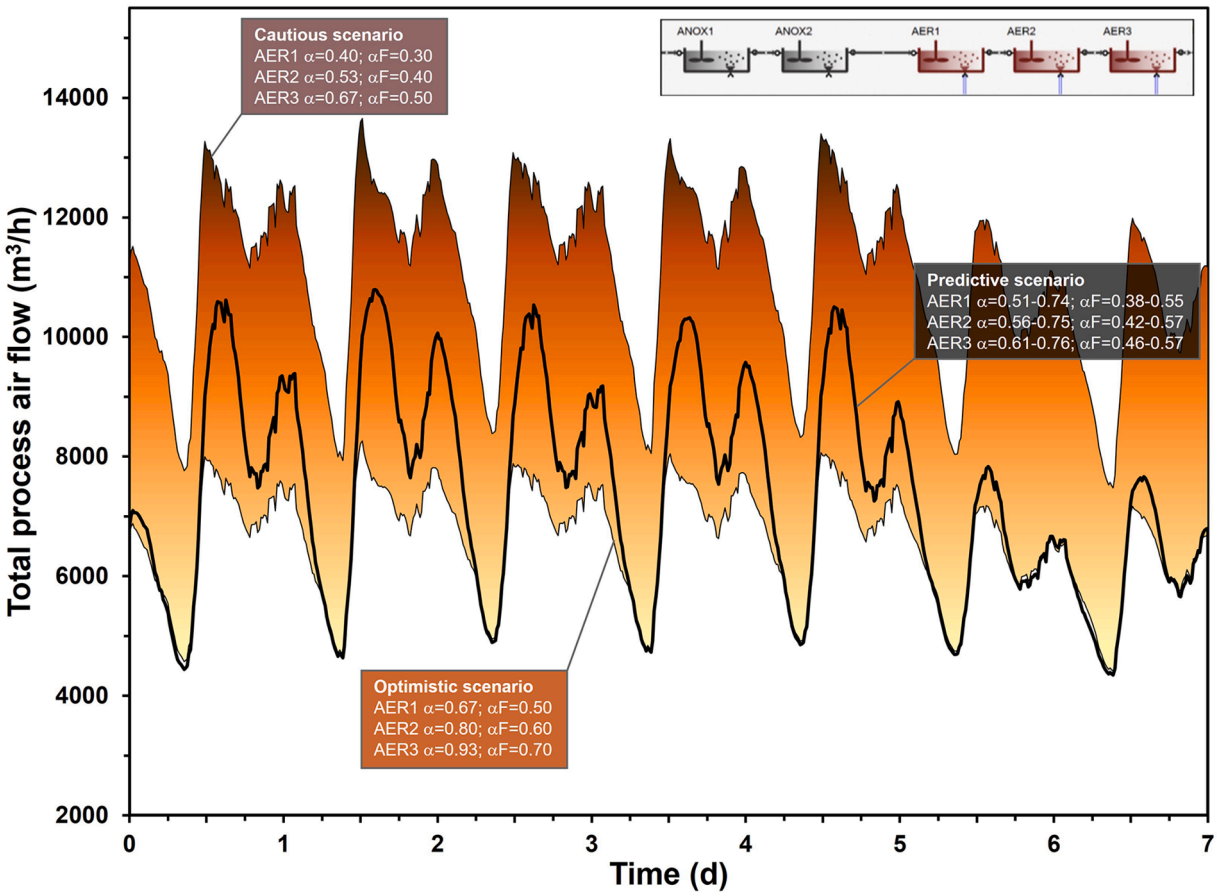

Fig. 7. Air flow comparison between constant and model-predicted αF-based design scenarios. Note how the dynamic α varies within the shaded area bounded by constant α sets (i.e., cases of cautious and optimistic).

to lack of sufficient air flow) leads to a violation of effluent limits.

Another scenario was also modelled, i.e. that of unscheduled additional loading of the same process. This is a case when even scheduled α values fall short of describing the true dynamic nature of the process. The model-predicted αF was compared to constant (labeled "passé") as well as a sinusoidal approximation used in the industry to schedule α values, illustrated in Fig. 9.

To fairly compare the calculation scenarios, the constant αF values assigned for the reactors in the passé scenario were averaged from weekday and weekend results of the predictive scenario. The sinusoidal

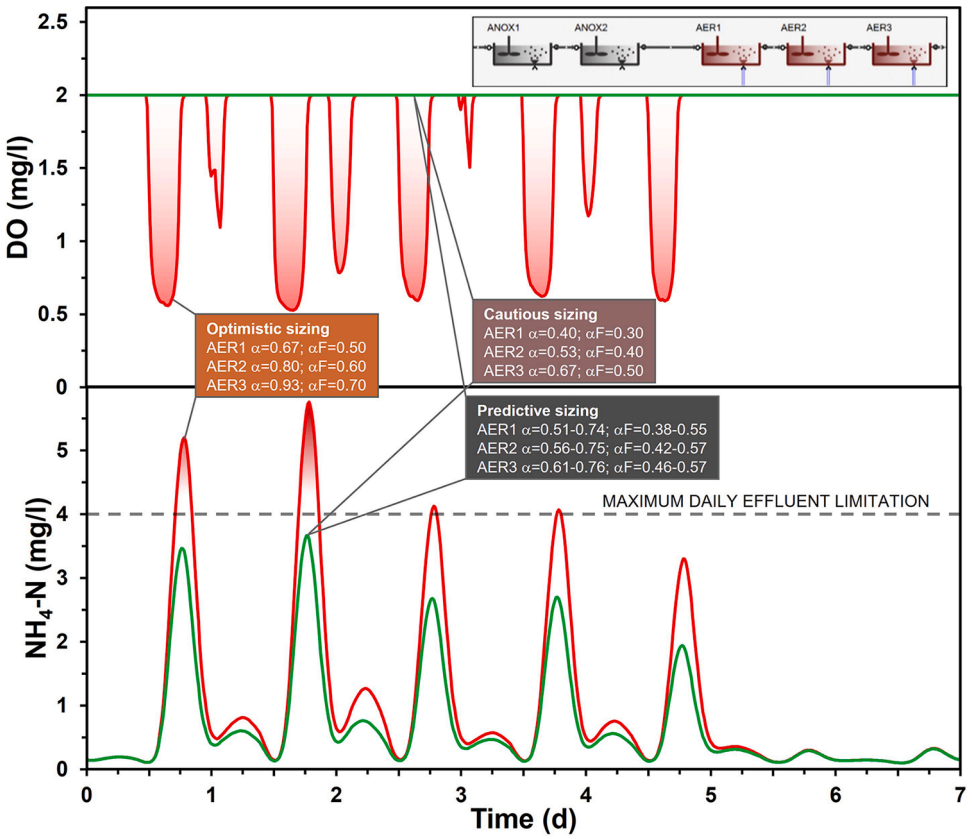

Fig. 8. DO and NH_4-N comparison with optimistic and model-predicted αF-based blower sizing.

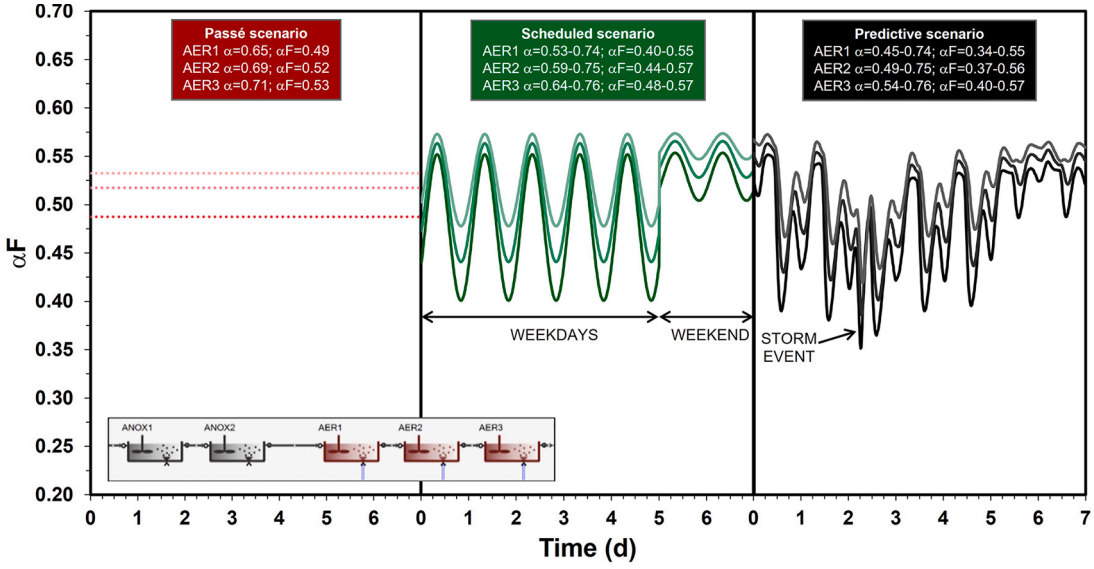

Fig. 9. Comparison of αF factor profiles by constant (passé), sinusoidal (scheduled), and model-predicted use cases.

approximation for αF in each reactor was created using a cosine function. Also, the sinusoidal αF variation was also based on the dynamically predicted model results by matching the average and the timing and value of the highest αF peak in each reactor separately for weekdays and weekend days. This choice simplifies the problem by assuming a single loading peak, whilst more complex α curves can be constructed by compounding sinusoidal functions so that the process loading pattern is mirrored in the α schedule.

After steady-state calculation and five weeks of dry weather loading, the model was run for a sixth week when an additional stormwater event was introduced to the plant on Wednesday doubling the peak flow. For the hydraulic loading, along with the load of organics and solids, N and P changed according to a first flush phenomenon. Air flow was modelled here, hence blower size was not restricted in these runs. Note that the sinusoidal αF scheduling, however, cannot change during the overload period. The modelled air flow, portrayed in Fig. 10, shows how the calculations based on constant or scheduled α are blind to the anomaly represented by the storm event on day 3. The predictive approach relies

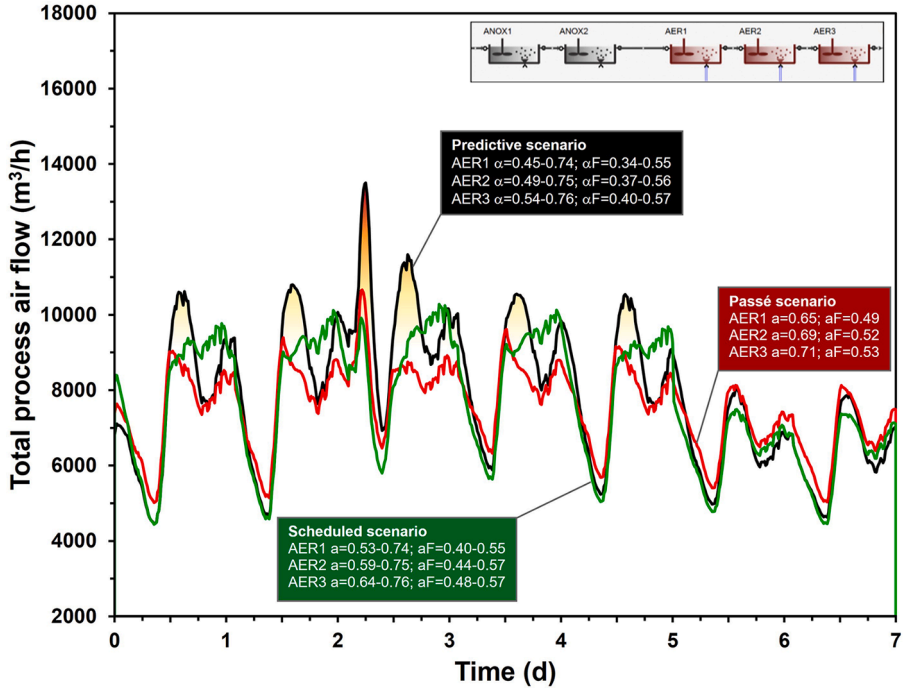

Fig. 10. Air flow comparison between constant (passé), sinusoidal (scheduled), and model-predicted αF scenarios; with overload.

on kinetic process calculations and considers the load increase, evaluates (properly) lower αF, and consequently, higher air flow demand ($1.35\ 10^4\ m^3\ h^{-1}$) associated with it. The sinusoidal and constant scenarios calculate that less air flow would suffice during this event – they do not account for the αF reduction by the sudden load variation – as seen previously in Fig. 9. The sinusoidal approach estimates a peak requirement of $1.03\ 10^4\ m^3\ h^{-1}$, less than the $1.07\ 10^4\ m^3\ h^{-1}$ suggested by the constant case, emphasizing that the predefined varying α values are randomly scheduled compared to actual loading events. These estimations are both more than 20% lower than what the dynamic alpha model predicts. There are even short lower-loaded periods during the weekend when the scheduled and passé scenarios overestimate the air consumption, supposing energy wastage compared to the predicted use case. Consequently, the overall blower energy consumption (35.4 MWh) summed for the predicted α-based run, despite the appropriately predicted increase during the storm event, is in fact, less than 4% higher than the demand associated with the sinusoidal and constant cases (34.5 MWh and 34.2 MWh, respectively). DO set points are maintained in all three scenarios, but, in reality, only a blower sized using the dynamic αF case would be able to maintain them through the entire time frame. Although the scheduled α is a step ahead of the constant α model, it is a time-dependent description of α but is not reliant on process dynamics. Hence, it cannot be considered a true dynamic model.

The presented dynamic α model is applicable to municipal mainstream treatment processes, with no separate model structure dedicated to address non-biodegradable surface-active agents (i.e., here only MLSS determines the asymptote of the maximum α factor in reactors). Certain types of industrial or mixed municipal-industrial wastewater may contain significant amounts of non-biodegradable surfactants. Thus, for such applications in the future, a new model component – representing non-biodegradables – shall be introduced, along with the necessary kinetic parameter re-estimation steps. Other potential further developments include adaptation to municipal sidestream processes.

6. Summary and conclusions

The proposed kinetic model concept for predicting the α factor in time and space was demonstrated to be an ideal option for dynamically estimating process air consumption of WRRFs under both dry and wet weather conditions. An α factor derived from process state variables is fundamentally different than a schedule of α values even though both appear time-dependent. This new predictive approach is verified to provide increased accuracy when sizing or improving aeration systems potentially resulting in significant operational and capital cost savings.

Model-predicted α values were revealed to provide a swift response in the calculated reactor-specific air flow consumption, reproducing the turn-up and turn-down effects that are important to take into account for time-related blower energy and cost estimation.

The prediction of αF factors using this method is advantageous compared to scheduling αF profiles manually, not only because it eliminates the need for complex knowledge and consideration about contributors (varying SRT, COD, MLSS etc.), but also because sudden operational changes in load may be accounted for using the underlying process variables. The concept can also be applied on a configuration to test whether a blower is undersized – if linked to process units with air flow restriction, and αF enters a low range that the blower capacity cannot handle, pointing out cases of effluent limit violation when DO falls short of target values.

The authors note that α generally correlates well with filtered COD in municipal influents based on the modelled facilities in this paper. However, the surfactant content relative to the filtered COD of certain wastewater samples may vary. If engineers have the opportunity to perform off-gas measurements in multiple locations of a system treating a given type of wastewater, it is advised that – based on air flow-weighted diurnal α and influent COD profiles – they re-estimate the "alpha improvement rate" and the filtered COD-alpha indicator regression parameters in order to achieve an α prediction more representative of that water type.

It shall be noted that the fouling effects on the αF factor are not modelled dynamically here because the longer term dynamic effects are outside the scope of this research. The authors advocate for closing this knowledge gap.

Future research shall be conducted to assess if the presented model represents the process water-associated dynamic nature of not only oxygen transfer but other gases, both in terms of absorption and stripping. Once sufficient data is available, surfactant elimination kinetics

may also be extended with temperature dependency.

CRediT authorship contribution statement

Dániel Bencsik: Methodology, Writing – original draft, Data curation. **Imre Takács:** Visualization, Supervision, Writing – review & editing. **Diego Rosso:** Visualization, Supervision, Software, Data curation, Writing – review & editing.

Declaration of Competing Interest

The authors declare that they have no known competing financial interests or personal relationships that could have appeared to influence the work reported in this paper.

Acknowledgements

The authors acknowledge water resource recovery facility operators and laboratory personnel who assisted in measurements required for model fitting. The authors also thank colleagues from Dynamita SARL (Tanush Wadhawan and Péter Budai) for their constructive feedback and technical assistance in carrying out simulation runs.

References

Ahmed, A.S., Khalil, A., Ito, Y., van Loosdrecht, M.C.M., Santoro, D., Rosso, D., Nakhla, G., 2021. Dynamic impact of cellulose and readily biodegradable substrate on oxygen transfer efficiency in sequencing batch reactors. Water Res. 190 https://doi.org/10.1016/j.watres.2020.116724.

Alex, J., Benedetti, L., Copp, J., Gernaey, K., Jeppsson, U., Nopens, I., Pons, M.N., Rieger, L., Rosén, C., Steyer, J.P., Vanrolleghem, P.A., Winkler, S., 2008. Benchmark Simulation Model no. 1 (BSM1). In: Report by the IWA Task Group on Benchmarking of Control Strategies for WWTPs, 19–20., ISBN: 9781843391463.

Amaral, A., Gillot, S., Garrido-Baserba, M., Filali, A., Karpinska, A.M., Plósz, B.G., De Groot, C., Bellandi, G., Nopens, I., Takács, I., Lizarralde, I., Jimenez, J.A., Fiat, J., Rieger, L., Arnell, M., Andersen, M., Jeppsson, U., Rehman, U., Fayolle, Y., Amerlinck, Y., Rosso, D., 2019. Modelling gas–liquid mass transfer in wastewater treatment: when current knowledge needs to encounter engineering practice and vice versa. Water Sci. Technol. 80 (4), 607–619. https://doi.org/10.2166/wst.2019.253.

American Society of Civil Engineers – ASCE, 2006. Measurement of Oxygen Transfer in Clean Water: ASCE Standard. ANSI/SEI 2-06. American Society of Civil Engineers, Reston, VA.

American Society of Civil Engineers – ASCE, 2018. Standard Guidelines for In-Process Oxygen Transfer Testing. ASCE/EWRI 18-18. American Society of Civil Engineers, Reston, VA.

Amerlinck, Y., De Keyser, W., Urchegui, G., Nopens, I., 2016. A realistic dynamic blower energy consumption model for wastewater applications. Water Sci. Technol. 74 (7), 1561–1576. https://doi.org/10.2166/wst.2016.360.

Aymerich, I., Rieger, L., Sobhani, R., Rosso, D., Corominas, L., 2015. The difference between energy consumption and energy cost: Modelling energy tariff structures for water resource recovery facilities. Water Res. 81, 113–123. https://doi.org/10.1016/j.watres.2015.04.033.

Baquero-Rodríguez, G.A., Lara-Borrero, J.A., Nolasco, D., Rosso, D., 2018. A critical review of the factors affecting modeling oxygen transfer by fine-pore diffusers in activated sludge. Water Environ. Res. 90 (5), 431–441. https://doi.org/10.2175/106143017x15131012152988.

Boog, J., Nivala, J., Kalbacher, T., van Afferden, Müller, R.A., 2020. Do wastewater pollutants impact oxygen transfer in aerated horizontal flow wetlands? Chem. Eng. J. 383, 123173 https://doi.org/10.1016/j.cej.2019.123173.

Doyle, M.L., Boyle, W.C., Rooney, T., Huibregtse, G.L., 1983. Pilot plant determination of oxygen transfer in fine bubble aeration. J. Water Pollut. Control Fed. 55 (12), 1435–1440.

Dynamita, 2021. Sumo21 User Manual. Dynamita SARL, Sigale, France.

Eckenfelder, W.W., Barnhart, E.L., 1961. The effect of organic substances on the transfer of oxygen from air bubbles in water. AlChE J. 7 (4), 631–634. https://doi.org/10.1002/aic.690070420.

Emami, N., Sobhani, R., Rosso, D., 2018. Diurnal variations of the energy intensity and associated greenhouse gas emissions for activated sludge processes. Water Sci. Technol. 77 (7), 1838–1850. https://doi.org/10.2166/wst.2018.054.

Garrido-Baserba, M., Asvapathanagul, P., McCarthy, G.W., Gocke, T.E., Olson, B.H., Park, H.D., Al-Omari, A., Murthy, S., Bott, C.B., Wett, B., Smeraldi, J.D., Shaw, A.R., Rosso, D, 2016. Linking biofilm growth to fouling and aeration performance of fine-pore diffuser in activated sludge. Water Res. 90, 317–328. https://doi.org/10.1016/j.watres.2015.12.011.

Garrido-Baserba, M., Asvapathanagul, P., Park, H.D., Kim, T.S., Baquero-Rodriguez, G.A., Olson, B.H., Rosso, D, 2018. Impact of fouling on the decline of aeration efficiency under different operational conditions at WRRFs. Sci. Total Environ. 639, 248–257. https://doi.org/10.1016/J.Scitotenv.2018.05.036.

Garrido-Baserba, M., Sobhani, R., Asvapathanagul, P., McCarthy, G.W., Olson, B.H., Odize, V., Al-Omari, A., Murthy, S., Nifong, A., Godwin, J., Bott, C.B., Stenstrom, M. K., Shaw, A.R., Rosso, D., 2017. Modelling the link amongst fine-pore diffuser fouling, oxygen transfer efficiency, and aeration energy intensity. Water Res. 111, 127–139. https://doi.org/10.1016/j.watres.2016.12.027.

Gillot, S., Capela-Marsal, S., Roustan, M., Heduit, A., 2005. Predicting oxygen transfer of fine bubble diffused aeration systems – model issued from dimensional analysis. Water Res. 39 (7), 1379–1387. https://doi.org/10.1016/j.watres.2005.01.008.

Gillot, S., Heduit, A., 2008. Prediction of alpha factor values for fine pore aeration systems. Water Sci. Technol. 57 (8), 1265–1269. https://doi.org/10.2166/wst.2008.222.

Henkel, J., Cornel, P., Wagner, M., 2011. Oxygen transfer in activated sludge – new insights and potentials for cost saving. Water Sci. Technol. 63 (12), 3034–3038. https://doi.org/10.2166/wst.2011.607.

Takacs, I., Patry, G.G., Nolasco, D., 1991. A dynamic model of the clarification-thickening process. Water Res. 25 (10), 1263–1271. https://doi.org/10.1016/0043-1354(91)90066-Y.

Jiang, L.M., Chen, L., Zhou, Z., Sun, D., Li, Y., Zhang, M., Liu, Y., Du, S., Chen, G., Yao, J., 2020. Fouling characterization and aeration performance recovery of fine-pore diffusers operated for 10 years in a full-scale wastewater treatment plant. Bioresour. Technol. 307, 123197 https://doi.org/10.1016/j.biortech.2020.123197.

Jiang, L.M., Garrido-Baserba, M., Nolasco, D., Al-Omari, A., De Clippeleir, H., Murthy, S., Rosso, D., 2017. Modelling oxygen transfer using dynamic alpha factors. Water Res. 124, 139–148. https://doi.org/10.1016/j.watres.2017.07.032.

Karpinska, A.M., Bridgeman, J., 2016. CFD-aided modelling of activated sludge systems – a critical review. Water Res. 88, 861–879. https://doi.org/10.1016/j.watres.2015.11.008.

Kessener, H., Ribbius, F., 1934. Comparison of aeration systems for the activated sludge process. Sewage Works J. 6 (3), 423–443.

Kim, Y., Boyle, W.C., 1993. Mechanisms of fouling in fine-pore diffuser aeration. J. Environ. Eng. 119 (6), 1119–1138. https://doi.org/10.1061/(ASCE)0733-9372(1993)119:6(1119).

Krampe, J., Krauth, K., 2003. Oxygen transfer into activated sludge with high MLSS concentrations. Water Sci. Technol. 47 (11), 297–303. https://doi.org/10.2166/wst.2003.0618.

Leu, S.Y., Rosso, D., Larson, L.E., Stenstrom, M.K., 2009. Real-time aeration efficiency monitoring in the activated sludge process and methods to reduce energy consumption and operating costs. Water Environ. Res. 81 (12), 2471–2781. https://doi.org/10.2175/106143009X425906.

Mueller, J.A., Kim, Y.K., Krupa, J.J., Shkreli, F., Nasr, S., Fitzpatrick, B., 2000. Full-scale demonstration of improvement in aeration efficiency. J. Environ. Eng. 126 (6), 549–555. https://doi.org/10.1061/(ASCE)0733-9372(2000)126:6(549).

Muller, E.B., Stouthamer, A.H., van Verseveld, H.W., Eikelboom, D.H., 1995. Aerobic domestic waste water treatment in a pilot plant with complete sludge retention by cross-flow filtration. Water Res. 29 (4), 1179–1189. https://doi.org/10.1016/0043-1354(94)00267-B.

Odize, V., Novak, J., Al-Omari, A., Rahman, A., Rosso, D., Murthy, S., De Clippeleir, H., 2016. Impact of organic carbon fractions and surfactants on oxygen transfer efficiency. In: Proceedings of the Water Environment Federation, pp. 3940–3947. https://doi.org/10.2175/193864716819713664.

Rieger, L., Gillot, S., Langergraber, G., Ohtsuki, T., Shaw, A., Takács, I., Winkler, S., 2013. Guidelines for Using Activated Sludge Models. IWA Publishing. Scientific and Technical Report No. 22., ISBN: 9781843391746.

Rosso, D., 2018. Aeration, Mixing, and Energy: Bubbles and Sparks. IWA Publishing. https://doi.org/10.2166/9781780407845. ISBN: 9781780407838.

Rosso, D., Iranpour, R., Stenstrom, M.K., 2005. Fifteen years of offgas transfer efficiency measurements on fine-pore aerators: key role of sludge age and normalized air flux. Water Environ. Res. 77 (3), 266–273. https://doi.org/10.2175/106143005X41843.

Rosso, D., Stenstrom, M.K., 2006a. Economic implications of fine-pore diffuser aging. Water Environ. Res. 78 (8), 810–815. https://doi.org/10.2175/106143006x101683.

Rosso, D., Stenstrom, M.K., 2006b. Surfactant effects on α-factors in aeration systems. Water Res. 40, 1397–1404. https://doi.org/10.1016/j.watres.2006.01.044.

Rosso, D., Stenstrom, M.K, 2007. Energy-saving benefits of denitrification. Environ. Eng. Appl. Res. Pract. 3, 1–11.

Schuchardt, A., Libra, J.A., Sahlmann, C., Wiesmann, U., Gnirss, R., 2007. Evaluation of oxygen transfer efficiency under process conditions using the dynamic off-gas method. Environ. Technol. 28 (5), 479–489. https://doi.org/10.1080/09593332808618812.

Steele, P., Rosso, D., Warner, R., 2019. More than hot air: full-scale efficiency comparison of jet aeration and coarse bubble aeration in aerobic digestion. In: Proceedings of the Water Environment Federation, pp. 4724–4734.

Stenstrom, M.K., Gilbert, R.G., 1981. Effects of alpha, beta and theta factor upon the design, specification and operation of aeration systems. Water Res. 15 (6), 643–654. https://doi.org/10.1016/0043-1354(81)90156-1.

U.S. Environmental Protection Agency – USEPA, 1989. Fine Pore (Fine Bubble) Aeration Systems. EPA/625/1-89/023. U.S. Environmental Protection Agency, Cincinnati, OH.

Wagner, M.R., Pöpel, H.J., 1996. Surface active agents and their influence on oxygen transfer. Water Sci. Technol. 34 (3-4), 249–256. https://doi.org/10.2166/wst.1996.0438.

Wagner, M.R., Pöpel, H.J., 1998. Oxygen transfer and aeration efficiency – influence of diffuser submergence, diffuser density, and blower type. Water Sci. Technol. 38 (3), 1–6. https://doi.org/10.1016/S0273-1223(98)00445-4.